

PAPER • OPEN ACCESS

## Selective liquid directional steering enabled by dual-scale reentrant ratchets



To cite this article: Jing Sun *et al* 2023 *Int. J. Extrem. Manuf.* **5** 025504

View the [article online](#) for updates and enhancements.

### You may also like

- [Transparent, self-cleaning and waterproof surfaces with tunable micro/nano dual-scale structures](#)  
Yujin Lee, Eun-Ah You and Young-Geun Ha
- [Fabrication of a 3D micro/nano dual-scale carbon array and its demonstration as the microelectrodes for supercapacitors](#)  
Shulan Jiang, Tielin Shi, Yang Gao et al.
- [Multiscale fabrication of biomimetic scaffolds for tympanic membrane tissue engineering](#)  
Carlos Mota, Serena Danti, Delfo D'Alessandro et al.

# Selective liquid directional steering enabled by dual-scale reentrant ratchets

Jing Sun<sup>1</sup> , Xuezhi Qin<sup>1</sup>, Yuxin Song<sup>1</sup>, Zhenyu Xu<sup>1</sup>, Chao Zhang<sup>1</sup>, Wei Wang<sup>2</sup>, Zhaokun Wang<sup>2</sup>, Bin Wang<sup>1,3,\*</sup> and Zuankai Wang<sup>2,\*</sup> 

<sup>1</sup> Department of Mechanical Engineering, City University of Hong Kong, Hong Kong 999077, People's Republic of China

<sup>2</sup> Department of Mechanical Engineering, The Hong Kong Polytechnic University, Hong Kong 999077, People's Republic of China

<sup>3</sup> Shenzhen Institute of Advanced Technology, Chinese Academy of Sciences, Shenzhen 518055, People's Republic of China

E-mail: [bwang55@cityu.edu.hk](mailto:bwang55@cityu.edu.hk) and [zk.wang@polyu.edu.hk](mailto:zk.wang@polyu.edu.hk)

Received 12 December 2022, revised 1 March 2023

Accepted for publication 13 April 2023

Published 27 April 2023



## Abstract

Achieving well-controlled directional steering of liquids is of great significance for both fundamental study and practical applications, such as microfluidics, biomedicine, and heat management. Recent advances allow liquids with different surface tensions to select their spreading directions on a same surface composed of macro ratchets with dual reentrant curvatures. Nevertheless, such intriguing directional steering function relies on 3D printed sophisticated structures and additional polishing process to eliminate the inevitable microgrooves-like surface deficiency generated from printing process, which increases the manufacturing complexity and severally hinders practical applications. Herein, we developed a simplified dual-scale structure that enables directional liquid steering via a straightforward 3D printing process without the need of any physical and chemical post-treatment. The dual-scale structure consists of macroscale tilt ratchet equipped with a reentrant tip and microscale grooves that decorated on the whole surface along a specific orientation. Distinct from conventional design requiring the elimination of microgrooves-like surface deficiency, we demonstrated that the microgrooves of dual-scale structure play a key role in delaying or promoting the local flow of liquids, tuning of which could even enable liquids select different spreading pathways. This study provides a new insight for developing surfaces with tunable multi-scale structures, and also advances our fundamental understanding of the interaction between liquid spreading dynamics and surface topography.

Supplementary material for this article is available [online](#)

Keywords: liquid spreading, reentrant ratchet, dual-scale structures

\* Authors to whom any correspondence should be addressed.



Original content from this work may be used under the terms of the [Creative Commons Attribution 4.0 licence](#). Any further distribution of this work must maintain attribution to the author(s) and the title of the work, journal citation and DOI.

## 1. Introduction

Controlling the directional transport of liquids on solid surfaces is essential for a variety of industry applications, ranging from oil-water separation, water harvesting, heat management to microfluidics [1–6]. Over the past decade, various strategies have been proposed to transport liquids to the preferential direction by taking advantage of external stimuli, including light, electricity, heat, force, and magnetic field, etc [7–12]. However, these approaches are also limited by their reliance on specific materials and the need for external energy input, which significantly restrict their broad-range applications. Intriguingly, many biological surfaces, such as the peristome of pitcher plants [13], the skin of lizard [14], and the spider silk [15], are found to be able to spontaneously and directionally transport liquid by virtue of their special surface topography and chemistry. In recent years, much attention has been paid to mimicking such kind of liquid transport by the control of asymmetric micro/nanostructures [16–18], wettability gradient [19, 20], and surface charge gradient [21].

Despite extensive progress, in previous studies, the spreading direction of liquids with different properties is dependent on the design of surfaces and cannot be tailored. Recent advances demonstrated that it is possible to make liquids with different surface tensions select their spreading direction on a same surface that consists of macroscale ratchets with transverse and longitudinal reentrant curvatures [22]. However, the realization of such intriguing liquid directional steering function required the combination of 3D printing and polishing treatment to eliminate the nonnegligible microgrooves-like surface deficiency generated from layer-by-layer printing process [23]. The additional polishing operation also increases the complexity of manufacturing and may damage the fine structures, which is unfavorable for practical applications. Therefore, it is necessary to simplify the surface topography and fabrication process while simultaneously maintaining the function of liquid directional steering.

In this work, we designed a simplified dual-scale structure that enables liquid directional steering via a straightforward 3D printing process without the need of any physical and chemical post-treatment. The dual-scale structure is macroscopically featured as tilt ratchet with a reentrant tip, and microscopically covered with grooves that arranged along a specific orientation, such as parallel or perpendicular to the tilt direction of ratchet. Distinct from conventional design that requires the elimination of the microgrooves-like surface deficiency, we experimentally and numerically demonstrate that the microgrooves serve to delay or promote the local flow of liquids, tuning of which could even steer the spreading direction of the same liquid. This study broadens our fundamental understanding of the interplay between liquid dynamics and multi-scale surface topography, and also provides an insight for designing surfaces to control complex fluidic process for many innovative applications.

## 2. Experiments and numerical simulation

### 2.1. Sample fabrication

The dual-scale reentrant ratchets were fabricated by a projection microstereolithography-based 3D printing system (microArch S130, BMF Nano Materials Technology Co., Ltd), and the printing material was an acrylic photosensitive resin that developed by the device manufacturer, called ‘HTL’, which is a high-performance engineering material with high strength, rigidity, and heat resistance. Before printing, a designed 3D model was first placed at certain orientation and sliced into cross-sectional images to generate the layers to be printed by using a slicing software (BMF Slicer), these images were later projected by an UV projector screen to be photocured in a layer-by-layer manner, the energy density of UV light, exposure time, and layer thickness are set as  $40 \text{ mW cm}^{-2}$ , 1.6 s,  $10 \mu\text{m}$ , respectively. Finally, the printed sample was cleaned by rinsing in ethanol for 15 min to remove residual photoresist, and air-dried in a fume hood before the use in experiments.

By making use of the layer-by-layer printing mode, we are able to fabricate object with tunable microscopic morphology by simply adjusting the printing parameters, for example, we fabricated the reentrant ratchets that covered with microgrooves perpendicular and parallel to the ratchet-tilting direction by merely modifying the placement orientation of a same model.

### 2.2. Sample characterizations and measurements

The surface morphology of dual-scale reentrant ratchets was revealed by an environmental scanning electron microscopy (ESEM, Quanta™ 250 FEG). The contact angle ( $\theta$ ) of liquids with different surface tensions was measured by using a drop shape analyzer system (DSA100, KRÜSS). To prepare liquids with different surface tensions, we varied the mass of ethanol added into water and magnetically stirred for 5 min, and then we measured the contact angle by gently depositing the liquid droplet with volume of  $\sim 1 \mu\text{l}$  on a flat surface with the same printing material as ratchets. The contact angles were determined by averaging three individual measurements.

The top-viewed macroscopic spreading process of liquids on the dual-scale ratchets was recorded by using a digital single-lens reflex camera (Nikon R5), where the liquids were dyed with blue ink for better clarification. The side-viewed and top-viewed microscopic spreading dynamics of liquids were captured by the drop shape analyzer (DSA100, KRÜSS) and an up-right microscope (VHX-1000, Keyence), respectively.

### 2.3. Numerical simulation

The simulation analysis of the liquid spreading on ratchet with perpendicular and parallel microgrooves was conducted in ANSYS Fluent. The numerical simulation captured the liquid–air interface movement by considering the volume of fluid

method, and the spreading distance of liquid was measured by ImageJ software.

### 3. Results and discussion

Figure 1(a) schematically illustrates the working mechanism of digital light processing-based 3D printing system, which subjects a vat of liquid resin to high-intensity light from a projector, and selectively cures the resin to a platform stage in a layer-by-layer process (figure 1(a)). Figure 1(b) shows the top and side-viewed scanning electron microscope (SEM) images of the as-printed periodically arranged reentrant ratchets, which are featured by A-shaped tilt islands with reentrant tip. The top and bottom width ( $w_1$ ,  $w_2$ ), length ( $L$ ), and tilting angle ( $\alpha$ ) of ratchet are 100  $\mu\text{m}$ , 400  $\mu\text{m}$ , 600  $\mu\text{m}$  and 45°, respectively. Figures 1(c) and (e) are the SEM images of two kinds of ratchets with identical macroscopic morphology, but distinct microgrooves that arranged perpendicular and parallel to the ratchet-tilting direction, respectively. The simplified dual-scale reentrant ratchets could realize liquids directional steering similar to that found on dual-curvature ratchets (figures S1 and S2), and tuning the geometric parameters such as top and bottom width, and layer thickness would also influence the spreading dynamics of liquids (figures S3 and S4). When continuously infusing water-ethanol mixtures on ratchets with perpendicular and microgrooves, we find that liquids exhibit different spreading dynamics. As shown in figures 2(a) and (c), the liquid mixture with ethanol mass fraction ( $f$ ) of 0.09 spreads forward along the ratchet-tilting direction on ratchets with perpendicular microgrooves (figure 2(a)), but flows backward on that with parallel microgrooves (figure 2(b)). Here  $f = m_e/(m_e + m_w)$ , with  $m_e$  and  $m_w$  being the mass of ethanol and water, respectively. As  $f$  increases from 0 to 1, the equilibrium contact angle ( $\theta$ ) of the liquid mixture on a printed flat surface decreases from  $\sim 70^\circ$  to  $\sim 10^\circ$  (figure S5), as for liquid with  $f$  of 0.09, the  $\theta$  is  $\sim 60^\circ$ . The variation of liquid transport distance with time is plotted in figure 2(c), where the positive and negative value of transport distance ( $X$ ) indicates forward and backward spreading, respectively.

To investigate the influence of microgrooves on the spreading dynamics of liquids with varying  $\theta$ , we plot the phase diagram that depicts the spreading direction of liquids on ratchets with parallel and perpendicular microgrooves, respectively. As shown in figure 2(d), liquids with  $\theta$  almost falling between  $\sim 40^\circ$  and  $\sim 60^\circ$  exhibit different spreading direction on these two kinds of ratchets, even as the tilt angle of ratchets  $\alpha$  increases from  $15^\circ$  to  $75^\circ$ . In contrast, liquids with larger or smaller  $\theta$  are not sensitive to the change of microgrooves and display the same spreading direction on both surfaces. Such a result implies that the orientation of microgrooves only plays a dominant role in regulating the spreading dynamics of liquids with moderate wettability, which can be attributed to the fact that liquids with relatively large  $\theta$  are hard to spread on these two kinds of microgrooves and thus the spreading dynamics is mainly determined by the macroscale structures, whereas liquids with small  $\theta$  spread too quickly to cover

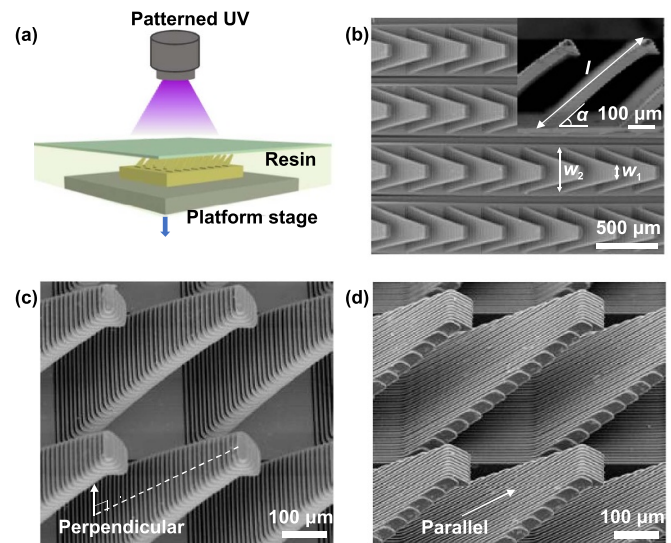


**Figure 1.** Design and fabrication of dual-scale reentrant ratchets. (a) Schematic illustration of digital light processing-based 3D printing setup. (b) Top and side-viewed scanning electron microscope (SEM) images of reentrant ratchets. (c, d) SEM image of reentrant ratchets with microgrooves arranged perpendicular and parallel to the ratchet-tilting direction, respectively.

the microgrooves and present bidirectional spreading on both surfaces.

To reveal the underlying mechanism of how microgrooves rectify the spreading regime of liquids, we recorded both the macroscopic and microscopic spreading process of liquids and focus on a typical case that liquid selects opposite spreading direction on ratchets with perpendicular and parallel microgrooves. Figure 3(a) shows the side-viewed snapshots of liquid with  $\theta$  of  $\sim 60^\circ$  spreads on ratchets ( $\alpha = 45^\circ$ ) with perpendicular microgrooves, and we define the time that we start to infuse liquid as  $t = 0$  s. With time progression, the left side of liquid remains pinned on the same ratchet that it initially makes contact, while the right side continuously flows forward along the ratchet-tilting direction. We further captured the microscopic spreading process of liquid on the right side by using an up-right microscope (VHX-1000, Keyence). As shown in figure 3(b), with the continuous infusion of liquid, the right side of liquid first maintains pinned at the reentrant tip of ratchets, as evidenced by the curved liquid front ( $t = 12$  s). However, the liquid eventually overcomes the pinning and jumps forward to next ratchet due to increased inner pressure ( $t = 14$  s). In contrast, on ratchets with parallel microgrooves, the same liquid with  $\theta$  of  $\sim 60^\circ$  exhibits an opposite spreading direction, with right side almost remain unchanged (figure 3(c)) and the left side continuous spreads backward. Microscopically, there is an evident precursor advancing ahead the left side of liquid, which fills the cavity between two rows of ratchets (figure 3(d)). In the meanwhile, the main liquid is first arrested by the top surface of ratchet and then gradually propagates atop it until makes contact with the precursor ( $t = 10$  s), which triggers the sudden jump of precursor to the next row of ratchet ( $t = 12$  s).



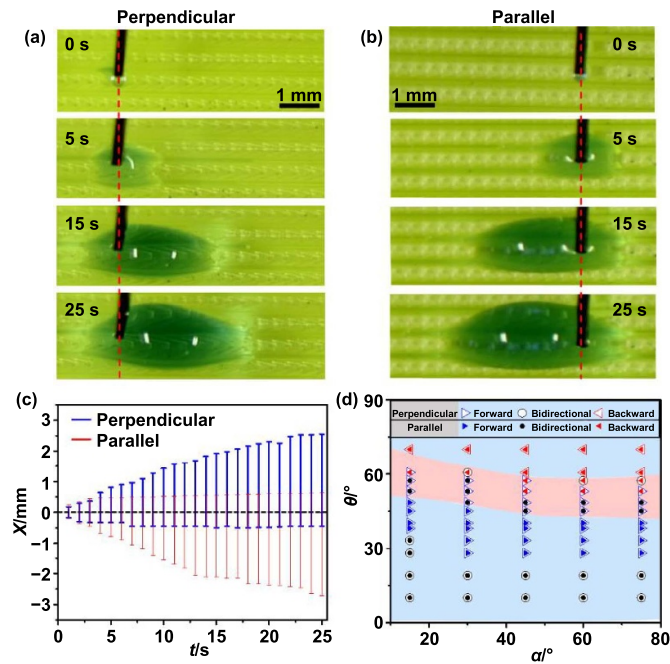


**Figure 2.** Liquids spreading dynamics on ratchets with perpendicular and parallel microgrooves. (a), (b) Snapshots of water/ethanol mixture (ethanol mass fraction  $f = 0.09$ ) spreads forward on ratchets with perpendicular microgrooves, spread backward on that with parallel microgrooves. (c) The variation of spreading distance  $X$  with time  $t$ , where the positive and negative value of  $X$  represent forward and backward spreading, respectively. (d) Phase map that depicts the spreading direction of liquids on ratchets with perpendicular and parallel microgrooves, respectively. Overall, liquids with  $\theta$  ranging from  $\sim 40^\circ$  to  $60^\circ$  exhibit different spreading direction on these two kinds of surfaces, as highlighted by the red area.

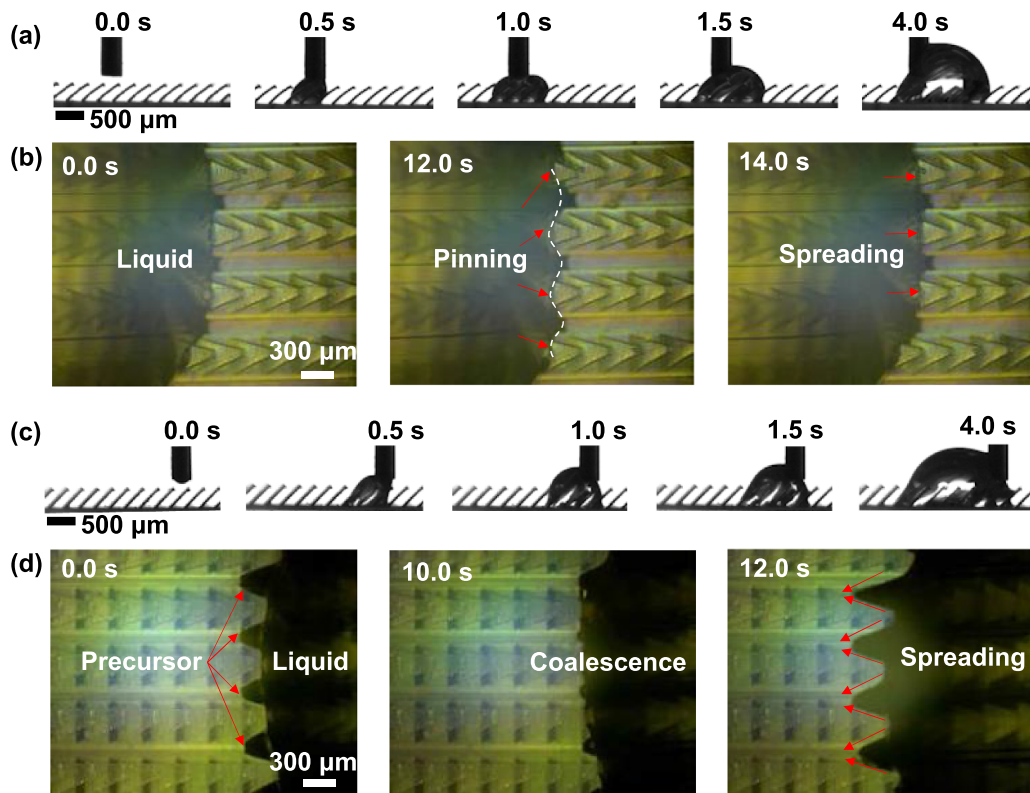


**Figure 3.** Macroscopic and microscopic spreading dynamics of liquids on ratchets with perpendicular and parallel microgrooves. (a), (b) Snapshots of the side and top view of liquid spreads on ratchets with perpendicular microgrooves, respectively. With time progression, the left side of liquid remains stay on the initially contacted ratchet whereas liquid on the right side continuous spreads forward upon overcoming the pinning at the reentrant tip of ratchet. (c), (d) Snapshots of the side and top view of liquid spreads on ratchets with parallel microgrooves, respectively. Liquid spreads backward instead on this surface. Microscopically, there is an apparent precursor advancing ahead of the liquid, upon contacting the precursor, liquid suddenly jumps backward to adjacent ratchet.

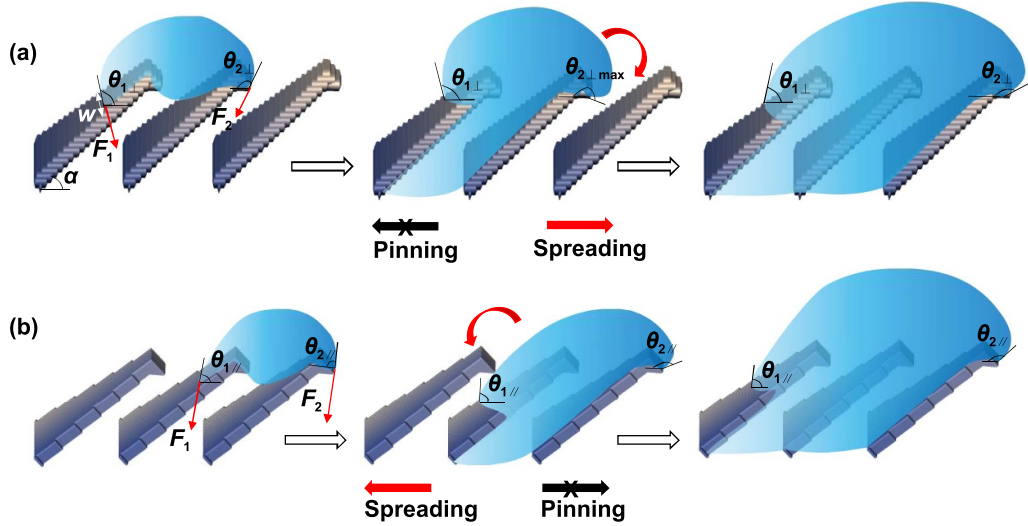


**Figure 4.** Mechanism of the differentiated spreading dynamics of liquids on ratchets with perpendicular and parallel microgrooves. (a) Schematics of forward spreading process of liquid on ratchets with perpendicular microgrooves. In this scenario, liquid was pinned by both step-like microgrooves and reentrant tip of ratchet, and first overcome the pinning at reentrant tip to spread along forward direction. (b) Schematics of backward spreading process of liquid on ratchets with parallel microgrooves. The liquid spreading along forward direction was inhibited by the reentrant tip, meanwhile, the spreading along backward direction was promoted by parallel microgrooves due to capillary wicking.

To understand the microscopic spreading dynamics of liquids, we theoretically analyze the variation of the local contact angles of liquids during the spreading on one row ratchets, as schematically shown in figures 4(a) and (b). For ratchets with perpendicular microgrooves, we consider the two boundary of the liquid on the side surface of ratchet and reentrant tip, with apparent contact angle depicted as  $\theta_{1\perp}$  and  $\theta_{2\perp}$ , respectively (figure 4(a)). Theoretically, with the infusion of liquid, both  $\theta_{1\perp}$  and  $\theta_{2\perp}$  will increase, with liquid pinned at the two boundaries, and the pinning of the solid–liquid–gas triple phase contact line at the corresponding boundary is maintained until the contact angle reaches a maximal value that can be described by the following geometrical boundary conditions [24, 25]:

$$\theta \leq \theta_{1\perp} \leq 90^\circ + \theta \quad (1)$$

$$90^\circ + \theta \leq \theta_{2\perp} \leq 180^\circ + \theta. \quad (2)$$

Here, the step-like microgrooves on the side surface of ratchet serve as multiple delay valves to slow down the backward spreading of liquid, whereas the reentrant tip serves to hinder the forward spreading of liquid. Thus, the spreading direction of liquids depends on the competition between the microgrooves ( $F_1$ ) and reentrant tip ( $F_2$ ), and the net force  $\Delta F_\perp$  along backward direction can be expressed as:

$$\Delta F_\perp = F_1 \cos \theta_{1\perp} + F_2 \cos (180^\circ - \theta_{2\perp}) \quad (3)$$

where  $F_1 = \gamma w$ ,  $F_2 = \gamma w_1$ ,  $\gamma$  is the surface tension of liquid and  $w$  is the width of ratchet at the position that liquid makes contact with side surface of ratchet,  $w_1 \leq w \leq w_2$ . It should note that, the pinning effect of microgrooves works more effective for liquids with relatively large  $\theta$  due to their slow spreading

speed, and liquids first break the pinning at reentrant tip with  $\theta_{2\perp}$  reaches the maximum (figure 4(a)), as exemplified by the fact that liquid with a  $\theta$  of  $\sim 60^\circ$  prefers to spread along forward direction.

In contrast, the parallel microgrooves serve to promote the spreading of liquids on the side surface of ratchet due to capillary wicking. In this scenario, the apparent contact angle  $\theta_{1\parallel}$  on the side surface and  $\theta_{2\parallel}$  at the reentrant tip should fall within the following range:

$$\alpha \leq \theta_{1\parallel} \leq \theta + \alpha \quad (4)$$

$$90^\circ - \alpha + \theta \leq \theta_{2\parallel} \leq 180^\circ + \theta. \quad (5)$$

The net force ( $\Delta F_\parallel$ ) exerted by parallel microgrooves and reentrant tip along backward spreading direction can also be expressed as the formation of equation (6), i.e.

$$\Delta F_\parallel = F_1 \cos \theta_{1\parallel} + F_2 \cos (180^\circ - \theta_{2\parallel}). \quad (6)$$

Considering that the maximum value of  $\theta_{1\parallel}$  is smaller than that of  $\theta_{1\perp}$ , we can expect that the parallel microgrooves provide larger driving force ( $F_1 \cos \theta_{1\parallel}$ ) along backward direction, which is thus beneficial for the backward spreading of liquids. Figure 4(b) schematically shows the backward spreading process of liquids. With the continuous infusion of liquid, both  $\theta_{1\parallel}$  and  $\theta_{2\parallel}$  increase until liquid propagates to make contact with adjacent ratchet on the left side, which triggers the backward spreading of liquid and what accompanied is the sudden decrease in  $\theta_{1\parallel}$  and  $\theta_{2\parallel}$  because of reduced inner pressure.

We resort to Fluent simulation to qualitatively verify the role of the microgrooves in regulating the spreading dynamics of liquids. Figures 5(a) and (b) show the simulated snapshots

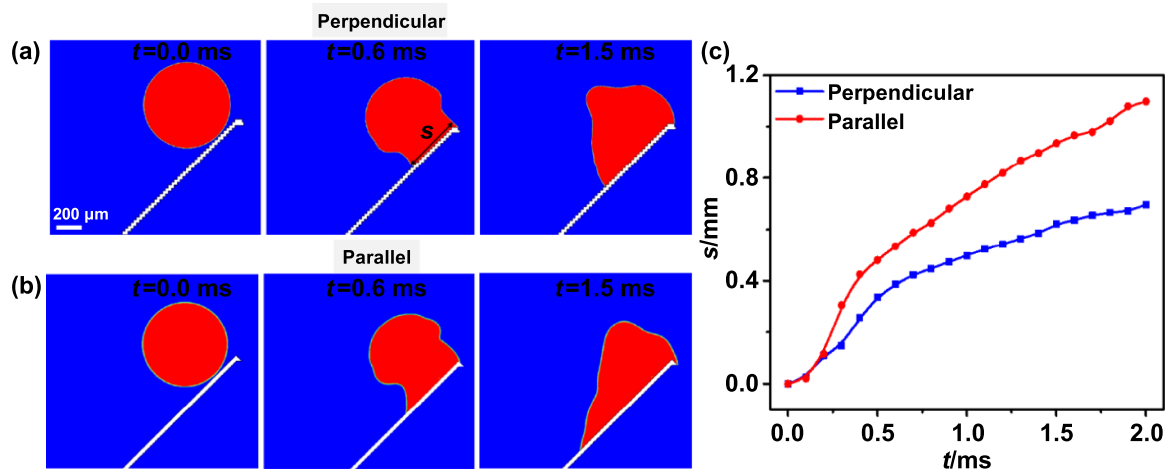


**Figure 5.** Simulation of liquid droplet spreading on ratchet with perpendicular and parallel microgrooves. (a), (b) Snapshots of the spreading process of a liquid droplet released on ratchet with perpendicular and parallel microgrooves, respectively. (c) Variation of spreading distance  $s$  with time  $t$ . Obviously, the  $s$  of liquid on ratchet with parallel microgrooves under identical timescale is larger than that on perpendicular microgroove, implying a smaller resistance for spreading on the ratchet with parallel microgroove.

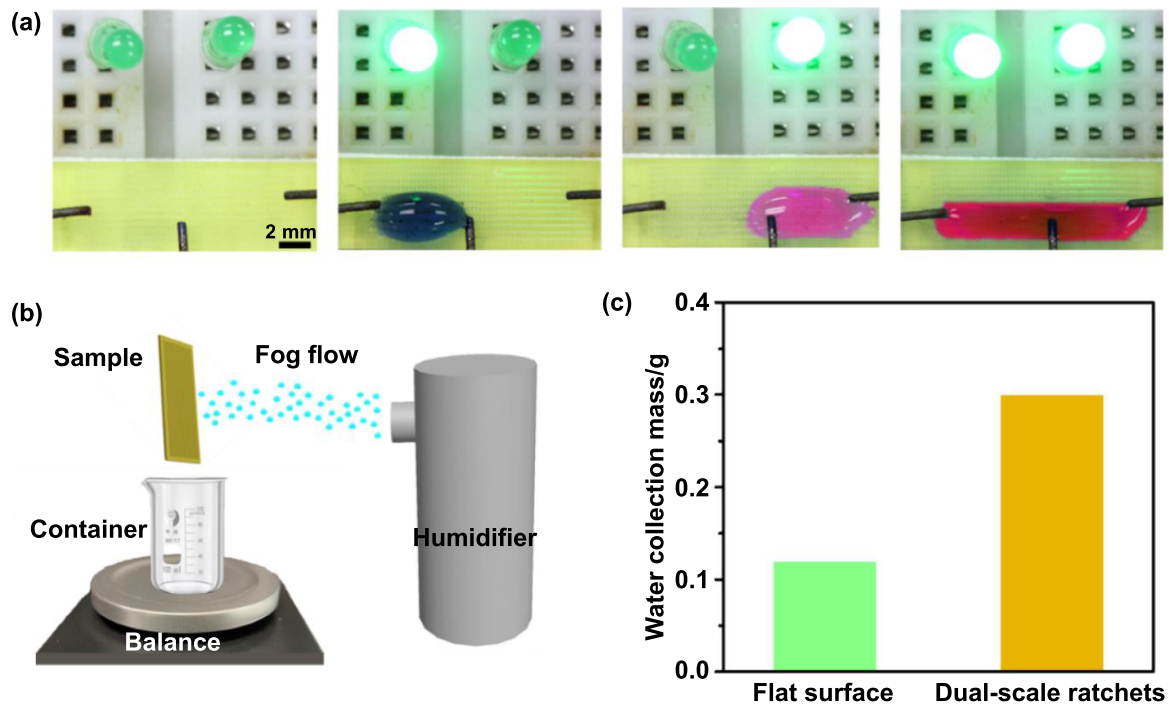


**Figure 6.** Demonstration of potential applications of the dual-scale reentrant ratchets. (a) Selectively lighting up the light-emitting diode by controlling the spreading direction of conductive liquids with different surface tensions on dual-scale reentrant ratchets. The conductive liquids that transport along backward, forward and bidirectional is mixture of  $\text{CuCl}_2$ , ethanol and water with mass fraction of 1:2:20, 1:7:20, and 1:14:20, respectively. (b) Schematic illustration of the fog collection setup, which is composed of a sample, a container, a balance, and a humidifier that produces a fog flow at a distance of  $\sim 10$  cm, the fog velocity is about  $25\text{--}30\text{ cm s}^{-1}$ . (c) Comparison of the collected water mass on flat surface and surface with dual-scale ratchets over 60 min.

of a liquid droplet released on ratchet with perpendicular and parallel microgrooves, respectively. At the initial contact with both ratchets, the contact base of liquid is similar, with time progression, there is an evident liquid advancing front appear on the ratchet with parallel microgrooves (figure 5(b)), and the spreading distance ( $s$ ) under identical timescale  $t$  remains larger than that on ratchet with perpendicular microgrooves (figure 5(c)), implying that liquid is easier to spread on the

ratchet with parallel microgroove, which is thus more favorable for the backward spreading. The surface tension and contact angle of liquid in this simulation was set as  $30\text{ mN m}^{-1}$  and  $20^\circ$ , respectively.

The unique property of the dual-scale reentrant structures holds great potential in various applications. Figure 6(a) shows that the ratchets with conducting liquids spreading along different directions can selectively lighting up light-emitting

diodes when used in electronic circuits. The conducting liquids consist of mixture of  $\text{CuCl}_2$ , ethanol and water with various mass fraction, and the spreading direction of conducting liquids can be tuned by changing the compositions and surface tensions of mixtures. Another application of the dual-scale ratchets is water harvesting. Previously, the groove structure has been found can promote droplets coalescence and accelerate the shedding of droplets [26], which is a promising structure for applications in fog collection. Figures 6(b) and (c) show that the dual-scale ratchets with parallel microgrooves significantly enhanced fog collection, on which the harvested water mass over 60 min is almost three folds of that on flat surface.

#### 4. Conclusion

In summary, we developed a simplified dual-scale structure to achieve well-controlled liquid directional steering via straightforward 3D printing, which eliminated the necessity of post-treatment in conventional design. The dual-scale structure consists of macroscale reentrant ratchet and microscale grooves that covered on the whole surface. We implemented experiments, theoretical analysis and numerical simulation demonstrated that the arrangement of microgrooves of the dual-scale reentrant ratchet could significantly rectify the spreading phase map of liquids. These results not only advance our fundamental understanding of the interaction between liquid spreading dynamics and complex surface topography, but also provide guidance for the design of surface for versatile practical applications, such as lab-on-chip devices, chemistry microreactors, and microfluidic systems.

#### Acknowledgments

We acknowledge the financial support from the ITF (GHP/021/19SZ), Shenzhen Science and Technology Innovation Council (9240061 and JCYJ20200109143206663), National Natural Science Foundation of China (No. 51975502), Research Grants Council of Hong Kong (No. C1006-20WF, No. 11213320), Science and Technology Planning Project of Guangdong Province (No. 2021A0505110002), Shenzhen-Hong Kong Joint Innovation Project (No. SGDX2019091716460172).

#### ORCID iDs

Jing Sun  <https://orcid.org/0000-0003-1905-5127>

Zuankai Wang  <https://orcid.org/0000-0002-3510-1122>

#### References

- [1] Yang Y, Li X J, Zheng X, Chen Z Y, Zhou Q F and Chen Y 2018 3D-printed biomimetic super-hydrophobic structure for microdroplet manipulation and oil/water separation *Adv. Mater.* **30** 1704912
- [2] Shi Z et al 2023 Constructing superhydrophobicity by self-assembly of  $\text{SiO}_2$ @polydopamine core-shell nanospheres with robust oil-water separation efficiency and anti-corrosion performance *Adv. Funct. Mater.* **33** 2213042
- [3] Park K C, Kim P, Grinthal A, He N, Fox D, Weaver J C and Aizenberg J 2016 Condensation on slippery asymmetric bumps *Nature* **531** 78–82
- [4] Q C Y et al 2021 Rapid and persistent suction condensation on hydrophilic surfaces for high-efficiency water collection *Nano Lett.* **21** 7411–8
- [5] Dudukovic N A, Fong E J, Gameda H B, DeOtte J R, Cerón M R, Moran B D, Davis J T, Baker S E and Duoss E B 2021 Cellular fluidics *Nature* **595** 58–65
- [6] Seemann R, Brinkmann M, Pfohl T and Herminghaus S 2012 Droplet based microfluidics *Rep. Prog. Phys.* **75** 016601
- [7] Li W, Tang X and Wang L 2020 Photopyroelectric microfluidics *Sci. Adv.* **6** eabc1693
- [8] McHale G, Brown C V, Newton M I, Wells G G and Sampara N 2011 Dielectrowetting driven spreading of droplets *Phys. Rev. Lett.* **107** 186101
- [9] Li J, Hou Y M, Liu Y H, Hao C L, Li M F, Chaudhury M K, Yao S H and Wang Z K 2016 Directional transport of high-temperature Janus droplets mediated by structural topography *Nat. Phys.* **12** 606–12
- [10] Noblin X, Kofman R and Celestini F 2009 Ratchetlike motion of a shaken drop *Phys. Rev. Lett.* **102** 194504
- [11] Zhang J Q, Wang X J, Wang Z Y, Pan S F, Yi B, Ai L Q, Gao J, Mugele F and Yao X 2021 Wetting ridge assisted programmed magnetic actuation of droplets on ferrofluid-infused surface *Nat. Commun.* **12** 7136
- [12] Hu S T, Cao X B, Reddyhoff T, Ding X J, Shi X, Dini D, deMello A J, Peng Z K and Wang Z K 2022 Pneumatic programmable superrepellent surfaces *Droplet* **1** 48–55
- [13] Chen H W, Zhang P F, Zhang L W, Liu H L, Jiang Y, Zhang D Y, Han Z W and Jiang L 2016 Continuous directional water transport on the peristome surface of *Nepenthes alata* *Nature* **532** 85–89
- [14] Comanns P, Buchberger G, Buchsbaum A, Baumgartner R, Kogler A, Bauer S and Baumgartner W 2015 Directional, passive liquid transport: the Texas horned lizard as a model for a biomimetic ‘liquid diode’ *J. R. Soc. Interface* **12** 20150415
- [15] Zheng Y M, Bai H, Huang Z B, Tian X L, Nie F Q, Zhao Y, Zhai J and Jiang L 2010 Directional water collection on wetted spider silk *Nature* **463** 640–3
- [16] Chu K H, Xiao R and Wang E N 2010 Uni-directional liquid spreading on asymmetric nanostructured surfaces *Nat. Mater.* **9** 413–7
- [17] Li J Q, Zhou X F, Li J, Che L F, Yao J, McHale G, Chaudhury M K and Wang Z K 2017 Topological liquid diode *Sci. Adv.* **3** eaao3530
- [18] Feng S L, Delannoy J, Malod A, Zheng H X, Quéré D and Wang Z K 2020 Tip-induced flipping of droplets on Janus pillars: from local reconfiguration to global transport *Sci. Adv.* **6** eabb4540
- [19] Chaudhury M K and Whitesides G M 1992 How to make water run uphill *Science* **256** 1539–41
- [20] Liu C R, Sun J, Li J, Xiang C H, Che L F, Wang Z K and Zhou X F 2017 Long-range spontaneous droplet self-propulsion on wettability gradient surfaces *Sci. Rep.* **7** 7552
- [21] Sun Q Q et al 2019 Surface charge printing for programmed droplet transport *Nat. Mater.* **18** 936–41
- [22] Feng S L, Zhu P G, Zheng H X, Zhan H Y, Chen C, Li J Q, Wang L Q, Yao X, Liu Y H and Wang Z K 2021 Three-dimensional capillary ratchet-induced liquid directional steering *Science* **373** 1344–8



- [23] Zhang Y, Wu L, Zou M M, Zhang L D and Song Y L 2022 Suppressing the step effect of 3D printing for constructing contact lenses *Adv. Mater.* **34** 2107249
- [24] Oliver J F, Huh C and Mason S G 1977 Resistance to spreading of liquids by sharp edges *J. Colloid Interface Sci.* **59** 568–81
- [25] Extrand C W and Moon S I 2008 Contact angles on spherical surfaces *Langmuir* **24** 9470–3
- [26] Bintein P B, Lhuissier H, Mongruel A, Royon L and Beysens D 2019 Grooves accelerate dew shedding *Phys. Rev. Lett.* **122** 098005